A highly soluble polyhedral oligomeric silsesquioxane end-capped perylenediimide dye

Xiao-Dong Zhuang, Yu Chen,* Bin Zhang, Yongxi Li, Bo Yu and Wenhan Qiao

Received (in Montpellier, France) 15th November 2009, Accepted 25th January 2010
First published as an Advance Article on the web 4th March 2010
DOI: 10.1039/b9nj00672a

A highly soluble perylenediimide (PDI) dye with unusual polyhedral oligomeric silsesquioxane (POSS) molecules was synthesized by the reaction of an aminopropylisobutyl POSS (POSS-NH_2) and 3,4,9,10-perylenetetracarboxylic dianhydride in the presence of $Zn(OAc)_2$. This material exhibits good thermal stability and high fluorescence quantum yield (Φ_F = 1.0). Its fluorescence time profile displays biexponential decay, with fluorescence lifetimes of 9.27 ± 0.26 ns (79.7%) and 2.55 ± 0.03 ns (20.3%). Molecular modelling results show that the lengths of the molecular long-axis and short-axis are about 3.5 and 2.2 nm, respectively. The values of the HOMO, LUMO, ionization potential and electron affinity estimated from the electrochemical data are −6.05, −3.75, 6.45 and 4.16 eV, respectively.

Introduction

Like the widely studied fullerenes and their organic/polymeric derivatives, perylene-3,4,9,10-bis(dicarboximides) are a subject of extensive academic and commercial interest as the active materials in organic/polymeric light-emitting diodes, organic-effect transistors, solar cells and molecular memory devices[1–12] due to their outstanding optical and electronic properties, structural flexibility, larger exciton diffusion lengths (30 ± 3 Å),[13] electron affinities (3.85 eV)[13] and molar absorption coefficients (58 000 M^{-1} cm^{-1} at 490 nm[14]). A thermally evaporated thin film of *N*,*N*′-ditridecyl-3,4,9,10-perylenetetracarboxylic diimide[15] annealed at 140 °C exhibits a high field-effect electron mobility of 2.1 cm^2 V^{-1} s^{-1}.

Basically, there are two ways to functionalize perylenediimides: one is incorporation of electron-donating or electron-withdrawing functional groups onto the perylene core,[16–20] the other is substitution at the N-atoms of the imide groups.[21–23] In the former case, the perylene core is found to be highly twisted because of electrostatic repulsion and steric encumbrance among the substituents.[16–20] Distortion of the conjugation and coplanarity of the perylene, and the increase of the intermolecular distance in perylene-based optoelectronic systems would hinder both intra- and intermolecular charge transfer processes, leading to a lower device performance. In a dispersed heterojunction solar cell device, both photocurrent generation and charge transport are functions of morphology, which is one of the most important issues affecting device performance. Although functionalization at the N-atoms of imide groups is a good synthetic method for keeping the planar structure of the perylene core unchanged, most of the materials synthesized by this approach have a relatively low solubility in common organic solvents, giving rise to great technical difficulty in the fabrication of large-area thin film devices by spin- or blade-coating solutions in organic solvents. In this case, these materials are usually thermally evaporated onto the substrates under high vacuum. There has thus been a continued pronounced interest in developing reliable and low-cost synthetic methods for preparing highly soluble planar perylenediimides.

A typical polyhedral oligomeric silsesquioxane (POSS) molecule,[24,25] represented by the formula ($R_8Si_8O_{12}$), consists of a rigid and cubic silica core with a 0.53 nm side length surrounded by eight organic corner groups, which endow the POSS molecule with higher reactivity and solubility in organic solvents. POSS molecules have been extensively incorporated into polymer matrixes to prepare soluble POSS-based hybrid materials, designed for optoelectronics and photonics applications, by chemical reactions or physical blending.[26–32] Here, we have designed and synthesized a highly soluble POSS end-capped perylenediimide (PDI) derivative (abbreviated as POSS-PDI-POSS), in which the bulky POSS molecules are chemically introduced to the N-atoms of the imide groups, as shown in Scheme 1.

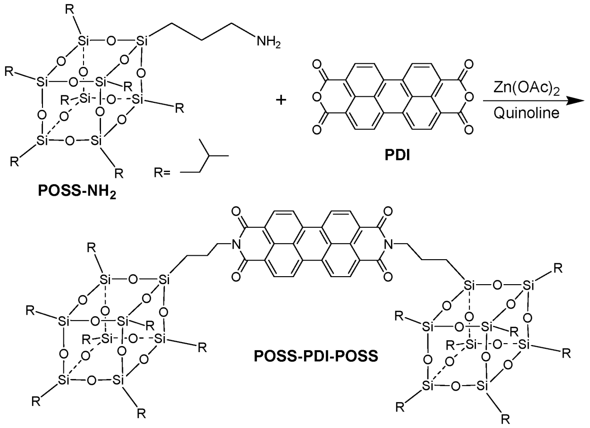

Scheme 1 Synthesis of POSS-PDI-POSS.

Key Laboratory for Advanced Materials, Department of Chemistry, East China University of Science and Technology, 130 Meilong Road, Shanghai 200237, China. E-mail: chentangyu@yahoo.com

Results and discussion

Substitution of the POSS molecules at the N-atoms of PDI can considerably improve the solubility and processibility of the parent material, and keep the planar structure of perylene core unchanged. After functionalization with POSS, the resultant material POSS-PDI-POSS exhibited high solubility in common organic solvents. However, it should be noted that the introduction of bulky end-capped substituents may limit the π–π stacking between pairs of perylenediimide units and consequently decrease the charge carrier mobility. The POSS used in this study has a flat profile of low absorbance over the ultraviolet–visible region, leading to its clear appearance. As expected, the UV/vis absorption spectrum (Fig. 1) of POSS-PDI-POSS in $CHCl_3$ exhibited a pattern typical of planar PDIs; four absorption peaks were located at 429, 458, 488 and 525 nm. The maxima bands at 525 and 488 nm correspond to the electronic S_0–S_1 and S_0–S_2 transitions,[33] respectively. For the PDI without substituents in the aromatic core, the maximum absorption wavelength was 526 nm.[34] This value is in good agreement with that which we observed in the UV/vis absorption spectrum of POSS-PDI-POSS in chloroform.

The fluorescence spectrum of POSS-PDI-POSS (Fig. 1) shows the mirror image of the corresponding UV/vis absorption bands, with a small Stokes shift (460 cm^{-1}), which indicates that the structural change between the ground state and the excited singlet state is small. Using rhodamine B[35,36] as a reference, which exhibited 0.9 of the fluorescence quantum yield (Φ_F) in ethanol upon 400 nm excitation, the Φ_F value of POSS-PDI-POSS measured in benzonitrile was about 1.0. The fluorescence time profile of the latter displayed biexponential decays, giving two fluorescence lifetimes of 9.27 ± 0.26 ns (79.7%) and 2.55 ± 0.03 ns (20.3%). Basically, for most perylene dyes with high fluorescence yields, their fluorescence time profiles have single exponential decays with lifetimes of about 4 ns, which seems to be in some disagreement with our observation. Is this material a mixture of mono- and bi-substituted compounds? To answer this question, we characterized its molecular structure by elemental analysis (EA) and NMR spectroscopy (including ^1H NMR, ^{13}C NMR and ^{29}Si NMR). As expected, the EA results were greatly consistent with the calculated values. The NMR results (Fig. 2) also supported the molecular structure of POSS-PDI-POSS. These findings implied that the obtained compound was indeed bi-substituted. Furthermore, we found that the photoluminescence peaks, as shown in Fig. 3, were gradually shifted to the red with increasing concentration due to re-absorption. This result is very common for perylene dyes because of their large oscillator strengths and their spectral overlaps between absorption and fluorescence bands. These findings suggested that re-absorption and re-emission could cause the dual-exponential effect, as we observed.

As shown in Fig. 4, the starting material 3,4,9,10-perylenetetracarboxylic dianhydride exhibited a very high thermal stability; its onset temperature for thermal bond cleavage was about 560 °C. Before 550 °C, POSS has completely decomposed; the residue was less than 2% at this temperature. POSS-PDI-POSS displayed two weight loss plateaus. At lower temperature, a weight loss of 5%, which can be assigned to the partial decomposition of alkyl chains in the molecular

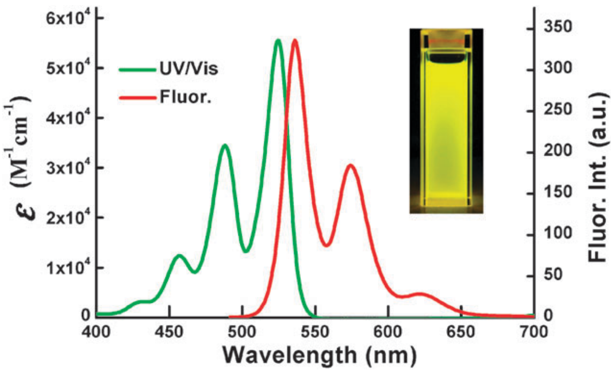

Fig. 1 UV/vis absorption spectrum (green line) and photoluminescence spectrum (red line, λ_{ex} = 488 nm) of POSS-PDI-POSS in $CHCl_3$ (1.0×10^{-5} M).

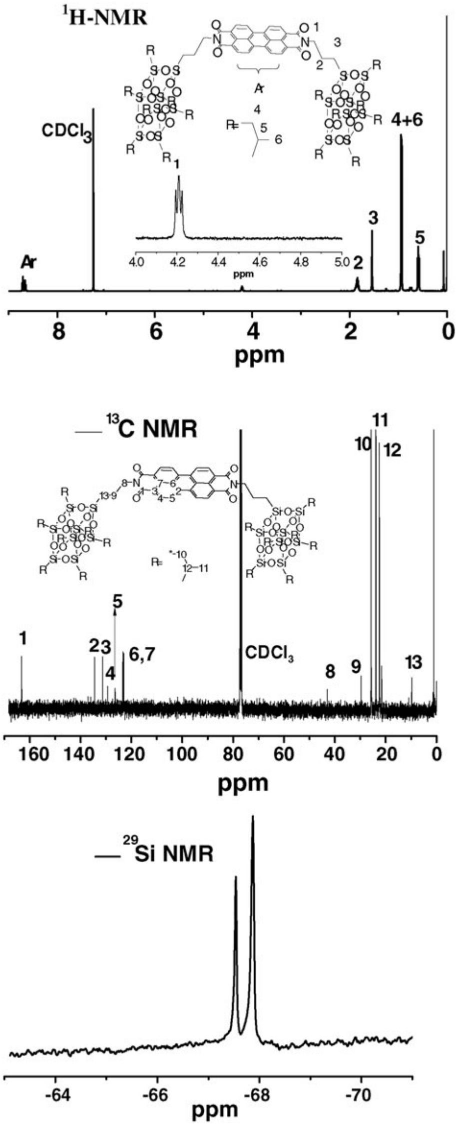

Fig. 2 NMR spectra of POSS-PDI-POSS in $CDCl_3$.

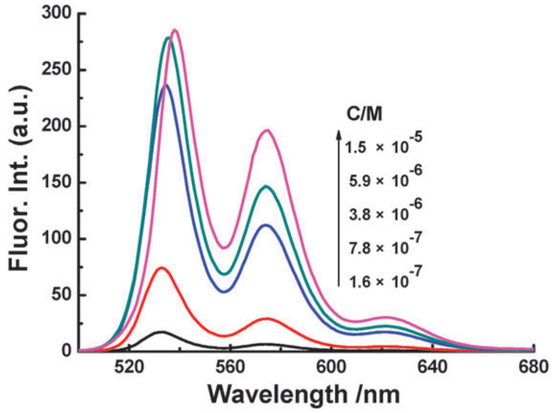

Fig. 3 Concentration dependence of the fluorescence spectra of POSS-PDI-POSS in $CHCl_3$.

structure of POSS, was observed. From the second weight loss plateau, the onset temperature was about 483 °C, leaving a residue of 32% at 600 °C. These results show that the resultant compound has a comparably good thermal stability.

Molecular modelling results showed that the lengths of the molecular long-axis and short-axis were about 3.5 and 2.2 nm, respectively. An AFM image of the monolayer Langmuir–Blodgett film of POSS-PDI-POSS (Fig. 5) exhibits an ordered arrangement, in which most of the long stripe-like species are on a micrometer scale in length and about 200 nm in width. The mean height of these species, except for a few larger aggregates, was about 3.2 nm, shorter than the length of the molecule's two-fold short-axes. These results suggest that in the Langmuir–Blodgett film, the molecules are predominantly oriented parallel to the molecular long-axes. The molecular planes are tilted with respect to the axis perpendicular to the mica surface by an angle of 24°.

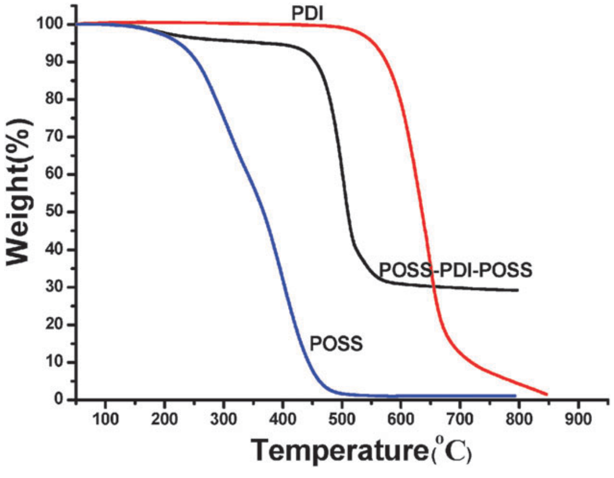

Fig. 4 TGA curves of the samples in flowing N_2 (100 mL min^{-1}).

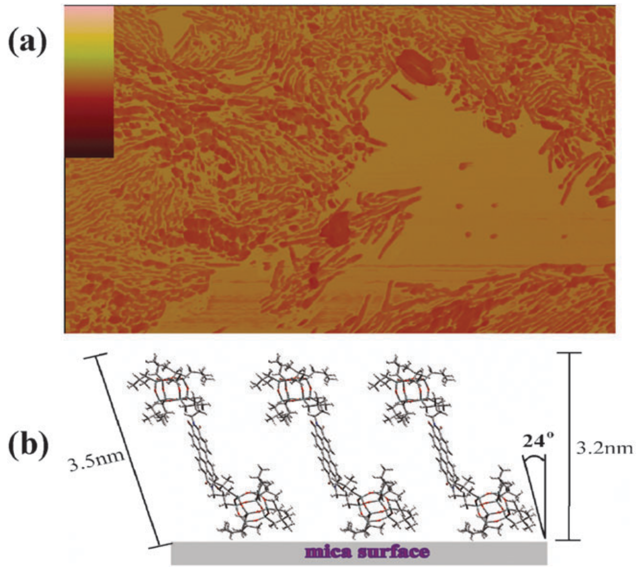

Fig. 5 (a) Surface patterns formed by POSS-PDI-POSS on the mica substrate. The 10 × 10 μm^2 AFM tapping mode amplitude image shows the structure of individual threads. (b) Molecular modelling configurations.

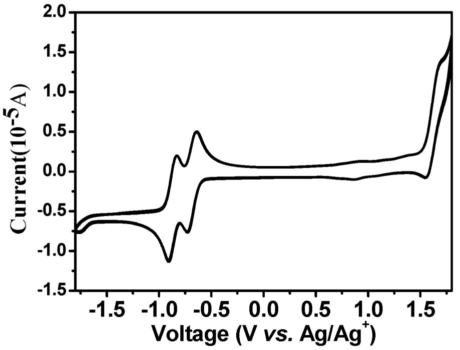

Fig. 6 Cyclic voltammogram of POSS-PDI-POSS in de-aerated CH_2Cl_2 containing Bu_4NClO_4 (0.1 M). Sweep rate: 20 mV s^{-1}.

Electrochemical measurements were carried out by cyclic voltammetry at a glassy carbon electrode in de-aerated CH_2Cl_2 containing 0.1 M Bu_4NClO_4 at room temperature (Fig. 6). The potentials were measured against a Ag/AgCl reference electrode. The redox values were found to be +1.65 and −0.64 V *vs.* Ag/AgCl, corresponding to the first oxidation and reduction potentials of POSS-PDI-POSS, respectively. Based on these data, the HOMO/LUMO could be calculated as −6.05 and −3.75 eV, respectively. The values of the ionization potential (IP) and electron affinity (EA)[37] were estimated as 6.45 and 4.16 eV, respectively. The HOMO–LUMO gap calculated by the electrochemical measurements was 2.30 eV, which is in good agreement with that estimated by the UV-Vis absorption onset data obtained in dilute solution ($E_g^{opt} = 1243.37/\lambda_{onset} = 1243.37/540 = 2.30$ eV).

Conclusions

An aminopropylisobutyl polyhedral oligomeric silsesquioxane ($POSS-NH_2$) was directly reacted with 3,4,9,10-perylenetetracarboxylic dianhydride to give a new highly soluble functional material, POSS-PDI-POSS. Molecular modelling results showed that the lengths of the molecular long-axis and short-axis were about 3.5 and 2.2 nm, respectively. This material showed a very high fluorescence quantum yield ($\Phi_F = 1.0$). Its fluorescence time profile exhibited biexponential decay, with lifetimes of 9.27 ± 0.26 ns (79.7%) and

2.55 ± 0.03 ns (20.3%). The HOMO and LUMO values, and the HOMO–LUMO gap, experimentally estimated by the onset of the redox potentials, were -6.05, -3.75 and 2.30 eV, respectively. It should be noted that the introduction of bulky end-capped substituents (*i.e.*, POSS) may limit π–π stacking between pairs of perylenediimide units and consequently decrease the charge carrier mobility. Therefore, some information about the distance between pairs of perylenediimide cores would be of particular interest. Further studies on these issues are currently in progress.

Experimental section

Materials and instruments

All chemicals were purchased from Aldrich and used without further purification. Organic solvents used in this study were purified, dried and distilled under dry nitrogen. An aminoisobutyl POSS (POSS-NH_2) was purchased from the Hybrid Plastics Company. The synthesis operations prior to the termination reaction were carried out under purified argon.

The UV/vis spectral measurements were carried out using a Shimadzu UV-2450 spectrophotometer. The thermal properties of the samples were measured using a Perkin-Elmer Pyris 1 thermogravimetric analyzer in flowing (100 mL min^{-1}) N_2. Steady-state fluorescence spectra were measured on a Shimadzu RF-5300 PC spectrofluorophotometer equipped with a photomultiplier tube with a high sensitivity in the 700–800 nm region. Samples for the fluorescence measurements were dissolved in dry chloroform, filtered, transferred to a long quartz cell, and then capped and bubbled with highly pure argon (without O_2 or moisture) for at least 15 min before measurement. NMR spectra were recorded on a Jeol Lambda 400 ($CDCl_3$ as solvent) instrument.

AFM topography images of monolayer Langmuir–Blodgett films on mica were obtained in constant repulsive force mode by an AFM (AJ-III, Aijian nanotechnology Inc., China) with a triangular micro-fabricated cantilever (Mikro Masch Co., Russia) with a length of 100 μm, a Si pyramidal tip and a spring constant of 48 N m^{-1}. A resonance frequency in the range 100–190 kHz was used, and resonance peaks in the frequency response of the cantilever, typically at 330 kHz, were chosen for the tapping mode oscillation. The AFM images were obtained with a scan range of 5×5 μm^2, and scanning frequencies were usually in the range 0.6–2.0 Hz per line. The measurements were carried out under ambient laboratory conditions. AFM images were obtained from at least five macroscopically-separated areas on each sample. At least two individual samples were prepared and imaged under the same conditions.

Cyclic voltammetry was performed on an ALS630B electrochemical analyzer in de-aerated CH_2CH_2 containing recrystallized Bu_4NClO_4 (0.1 M) as a supporting electrolyte at 298 K. A conventional three-electrode cell was used with a platinum working electrode (surface area of 0.3 mm^2) and a platinum wire as the counter-electrode. The Pt working electrode was routinely polished with BAS polishing alumina suspension and rinsed with acetone before use. The measured potentials were recorded with respect to the Ag/AgCl (0.01 M) reference electrode. All electrochemical measurements were carried out under an atmospheric pressure of argon.

Theoretical calculations

Geometry optimisations were carried out using the B3LYP functional and 6-31G basis set with the unrestricted Hartree–Fock (UHF) formalism, as implemented in the Gaussian 03 program, revision C.02. Graphical outputs of the computational results were generated using the Gauss View software program (version 3.09) developed by Semichem, Inc.

Synthesis of POSS-PDI-POSS

A mixture of 3,4,9,10-perylenetetracarboxylic dianhydride (90 mg, 0.23 mmol), aminopropylisobutyl-POSS (POSS-NH_2, 0.5 g, 0.57 mmol), anhydrous $Zn(OAc)_2$ (100 mg, 0.55 mmol) and dry quinoline (50 g) were stirred at 190 °C for 24 h under a highly purified argon atmosphere, and then cooled to room temperature. The solvent was removed by distillation under reduced pressure, leaving a red residue, which was chromatographed on silica gel using a gradient of toluene and chloroform in order to remove the largest portion of polar impurities. The red fraction ($R_f = 0.33$ in toluene) was collected. After evaporation of the solvent, 267 mg of red solid POSS-PDI-POSS (55% yield) was obtained. ^1H NMR (400 MHz, $CDCl_3$): δ (ppm) = 8.67 (d, 4H, perylene-*H*), 8.71–8.73 (d, 4H, perylene-*H*), 4.22 (t, 4H, $-CH_2-$), 1.85 (m, 18H, –CH– and Si–CH_2–CH_2–), 0.94 (d, 84H, $-CH_3$), 0.60 (t, 32H, Si–CH_2–). ^{13}C NMR (75 MHz, $CDCl_3$): δ (ppm) = 163.2, 134.5, 131.3, 129.4, 126.4, 123.4, 123.0, 42.9, 29.7, 25.7, 23.9, 22.5, 21.6, 9.8. ^{29}Si NMR (59.4 MHz, $CDCl_3$): δ (ppm) = -67.5, -67.8.[38] Elemental analysis: calc. for $C_{86}H_{146}N_2O_{28}Si_{16}$: C, 49.06; H, 6.99; N, 1.33%. Found: C, 49.10; H, 7.29; N; 1.12%.

Acknowledgements

We are grateful for the financial support of National Natural Science Foundation of China (20676034, 20876046), the Ministry of Education of China (309013) and Shanghai Municipal Educational Commission for the Shuguang fellowship (08GG10) and Shanghai Eastern Scholarship, respectively.

References

1 P. Ranke, I. Bleyl, J. Simmerer, D. Haarer, A. Bacher and H. W. Schmidt, *Appl. Phys. Lett.*, 1997, **71**, 1332–1334.
2 C. W. Struijk, A. B. Sieval, J. E. J. Dakhorst, M. van Dijk, P. Kimkes, R. B. M. Koehorst, H. Donker, T. J. Schaafsma, S. J. Picken, A. M. van de Craats, J. M. Warman, H. Zuilhof and E. J. R. Sudhölter, *J. Am. Chem. Soc.*, 2000, **122**, 11057–11066.
3 S. Liu, G. Sui, R. A. Cormier, R. M. Leblanc and B. A. Gregg, *J. Phys. Chem. B*, 2002, **106**, 1307–1315.
4 B. A. Jones, M. J. Ahrens, M. H. Yoon, A. Facchetti, T. J. Marks and M. R. Wasielewski, *Angew. Chem., Int. Ed.*, 2004, **43**, 6363–6366.
5 Y. Che, X. Yang, S. Loser and L. Zang, *Nano Lett.*, 2008, **8**, 2219–2223.
6 F. Würthner, *Chem. Commun.*, 2004, 1564–1579.
7 H. E. Katz, A. J. Lovinger, J. Johnson, C. Kloc, T. Siegrist, W. Li, Y.-Y. Lin and A. Dodabalapur, *Nature*, 2000, **404**, 478–481.
8 A. Babel and S. A. Jenekhe, *Adv. Mater.*, 2002, **14**, 371–374.
9 A. S. Lukas, P. J. Bushard and M. R. Wasielewski, *J. Am. Chem. Soc.*, 2001, **123**, 2440–2441.

10 F. Würthner, V. Stepanenko, Z. Chen, C. R. Saha-Moeller, N. Kocher and D. Stalke, *J. Org. Chem.*, 2004, **69**, 7933–7939.

11 A. S. Lukas, Y. Zhao, S. E. Miller and M. R. Wasielewski, *J. Phys. Chem. B*, 2002, **106**, 1299–1306.

12 A. Babel and S. A. Jenekhe, *J. Phys. Chem. B*, 2002, **106**, 6129–6132.

13 P. R. L. Malenfant, C. D. Dimitrakopoulos, J. D. Gelorme, L. L. Kosbar, T. O. Graham, A. Curioni and W. Andreoni, *Appl. Phys. Lett.*, 2002, **80**, 2517–2519.

14 R. S. Loewe, K. Y. Tomizaki, F. Chevalier and J. S. Lindsey, *J. Porphyrins Phthalocyanines*, 2002, **6**, 626–642.

15 S. Tatemichi, M. Ichikawa, T. Koyama and Y. Taniguchi, *Appl. Phys. Lett.*, 2006, **89**, 112108.

16 J. Baffreau, S. Leroy-Lhez, N. Van Anh, R. M. Williams and P. Hudhomme, *Chem.–Eur. J.*, 2008, **14**, 4974–4992.

17 S. Leroy-Lhez, J. Baffreau, L. Perrin, E. Levillain, M. Allain, M.-J. Blesa and P. Hudhomme, *J. Org. Chem.*, 2005, **70**, 6313–6320.

18 Y. Li, L. Tan, Z. Wang, H. Qian, Y. Shi and W. Hu, *Org. Lett.*, 2008, **10**, 529–532.

19 Z. Chen, M. G. Debije, T. Debaerdemaeker, P. Osswald and F. Würthner, *ChemPhysChem*, 2004, **5**, 137–140.

20 H. Graaf, W. Michaelis, G. Schnurpfeil, N. Jaeger and D. Schlettwein, *Org. Electron.*, 2004, **5**, 237–249.

21 J. Locklin, D. Li, S. C. B. Mannsfeld, E. J. Borkent, H. Meng, R. Advincula and Z. Bao, *Chem. Mater.*, 2005, **17**, 3366–3374.

22 E. Peeters, P. A. van Hal, S. C. J. Meskers, A. J. Janssen and E. W. Meijer, *Chem.–Eur. J.*, 2002, **8**, 4470–4474.

23 H. Langhals, R. Ismael and O. Yürük, *Tetrahedron*, 2000, **56**, 5435–5441.

24 M. K. Kolel-Veetil, D. D. Dominguez and T. M. Keller, *J. Polym. Sci., Part A: Polym. Chem.*, 2008, **46**, 2581–2587.

25 R. H. Baney, M. Itoh, A. Sakakibara and T. Suzuki, *Chem. Rev.*, 1995, **95**, 1409–1430.

26 W. Zhang, L. Liu, X. Zhuang, X. Li, J. Bai and Y. Chen, *J. Polym. Sci., Part A: Polym. Chem.*, 2008, **46**, 7049–7061.

27 W. Zhang, X. Zhuang, X. Li, Y. Lin, J. Bai and Y. Chen, *React. Funct. Polym.*, 2009, **69**, 124–129.

28 A. Romo-Uribe, P. T. Mather, T. S. Haddad and J. D. Lichtenhan, *J. Polym. Sci., Part B: Polym. Phys.*, 1998, **36**, 1857–1872.

29 N. Amir, A. Levina and M. S. Silverstein, *J. Polym. Sci., Part A: Polym. Chem.*, 2007, **45**, 4264–4275.

30 D. B. Drazkowski, A. Lee, T. S. Haddad and D. J. Cookson, *Macromolecules*, 2006, **39**, 1854–1863.

31 J. D. Lichtenhan, Y. A. Otonari and M. J. Cam, *Macromolecules*, 1995, **28**, 8435–8437.

32 V. Castelvetro, F. Ciardelli, V. C. De and A. Puppo, *Macromol. Rapid Commun.*, 2006, **27**, 619–625.

33 S. Chen, Y. Liu, W. Qiu, X. Sun, Y. Ma and D. Zhu, *Chem. Mater.*, 2005, **17**, 2208–2215.

34 F. Würthner, *Chem. Commun.*, 2004, 1564–1579.

35 C. de Mello Donegá, S. G. Hickey, S. F. Wuister, D. Vanmaekelbergh and A. Meijerink, *J. Phys. Chem. B*, 2003, **107**, 489–496.

36 X. Zhong, S. Liu, Z. Zhang, L. Lin, Z. Wei and W. Knoll, *J. Mater. Chem.*, 2004, **14**, 2790–2794.

37 J. Pei, J. Ni, X. Zhou, X. Cao and Y. Lai, *J. Org. Chem.*, 2002, **67**, 8104–8113.

38 T. Hirai, M. Leolukman, S. Jin, R. Goseki, Y. Ishida, M. Kakimoto, T. Hayakawa, M. Ree and P. Gopalan, *Macromolecules*, 2009, **42**, 8835–8843.